Journal of Chemical Health Risks

www.jchr.org

JCHR (2024) 14(4), 2187-2195 | ISSN:2251-6727

Hybrid Wavelength and Time Division Multiplexed High-Capacity Inter-Satellite Optical Wireless System

Jayalani M[1], Jaheer Ushen S[2], Janarthanan J[3], Vignesh S[4]

[1]Assistant Professor , [2,3,4]Final Year B.E. ECE, Department of Electronics and Communication Engineering, Al-Ameen Engineering College (Autonomous), Erode – 638 104, Tamilnadu, India

(Received: 16 June 2024 Revised: 11 July 2024 Accepted: 11 August 2024)

KEYWORDS
optical communication, free spacequantum, IR photodetector; wirelesscommunication, cascade laser;

ABSTRACT:

The greatest choice for greater reach and data speeds is to combine optical code division multiplexed with fso communication. The impact of atmospheric conditions on the strength of absorbed radiation is investigated in this study, both empirically and conceptually. It is suggested to build a laboratory test stand for the FSO system that operates in the third-atmosphere propagation window (8–12 m). The experimental analysis was then carried out in both a laboratory and in real-world situations, taking into account various atmospheric variables. The observations were implemented in two optical lines with lengths of 1.5 m and 10 m, respectively.In the situation of limited visibility (e.g., light rain and fogs), it was discovered that optical light with a wavelength of around 10 m has superior transmission qualities than near-infrared wavelengths. Analytical investigations came to the same result. Quantum cascade laser and HgCdTe photodiodes, for example. We are mostly interested in outdoor terrestrial OWC networks that operate in the near-IR spectrum. In the literature, this is known to as FSO communication. FSO devices are used to communicate at a high rate between two fixed sites across long distances of many kilometres. FSO lines offer a substantially greater optical bandwidth than their radio-frequency (RF) equivalents, allowing much faster data speeds.

Introduction:

The rise of wireless technology is the most major technological movements in history. Digital network and gadgets are spread much more quickly than anyone could have expected 30 years ago, and they will continue to be a vital element of modern society for the near future. M. Uysal's work is presently supported by the Marie Curie Global Reintegration Grant and the TUBITAK Grant 111E143. The term "wireless" has become practically synonymous with RF)technology as a result of the extensive deployment and use of wireless RF systems and devices. The RF band, on the other hand, is essentially constricted because most sub-bands of the visible radiation have limited capacity and are expensive.

. The demand for radio frequency spectrum is outstripping supply, thus it's time to look into other options for wireless technology in the higher frequencies of the electromagnetic radiation. OWC is use of optical particles in unguided propagation mediums such as visible, infrared, and ultraviolet (UV) bands. Signaling with lighthouse fires, fog, ship flags, and telegraph telegraph were all used in the past [1]. Sunlight has been used for long-distance communication since prehistoric times. First use of sunlight for communications is credited to the ancient Romans, who used their polished shields to send messages by reflecting light during battles [2].

. Although the heliograph was designed for geodetic survey, throughout the 19th century and early 20th century, it was commonly used for military purposes. Alexander Graham Bell invented the photophone in 1880, which is frequently referred to as the world's first mobile telephone system. It was based on speech-induced vibrations in a mirror at the transmitter. The vibrations were reflected and projected by the sun, and then transformed back into sound at the receiver. Although it was never marketed, Bell described the photophone as "the greatest innovation [he] had ever developed, greater than the phone" [3].

In the modern sense, OWC uses lasers or LEDs as transmitters. MIT Lincoln Labs created an experimental

Journal of Chemical Health Risks
www.jchr.org
JCHR (2024) 14(4), 2187-2195 | ISSN:2251-6727

OWC link in 1962 that used a light emitting GaAs diode to transmit TV signals over a range of 30 miles. Following the advent of the laser, OWC was envisaged as a significant deployment location for lasers, and various tests 2 were conducted. Bell Labs scientists used a ruby laser to send signals 25 kilometres away just months after the first public announcement of a working laser in July 1960 [5].

[6] is a complete list of OWC experiments that took place between 1960 and 1970 and used a variety of lasers and modulation techniques. The results were typically poor due to substantial divergence of laser beams and inability to cope with air disturbances. After its emergence in the 1970s, low-loss fibre optics became the obvious choice for long-distance optical transmission, and the focus shifted away from OWC systems. OWC has mostly been employed for covert military reasons [7], [8], and aerospace engineering like inter-satellite and deep-space links1 over the years. OWC's mainstream market penetration has been limited, apart from IrDA, which has become a very efficacy and quality short-range transmission solution [16].

Two optical lines with wavelengths of 1.5 and 10 m were investigated. The realised bit error rate (BER) [27] was used to assess transmission quality. When compared to near-infrared waves, a wavelength of roughly 10 m was shown to have better transmission qualities in the situation of restricted sight. In traditional transmission channels, similar circumstances involving the selection/determination of acceptable characteristics of the sources of signals being delivered across noisy transmission channels to increase transmission efficiency also occur.

2. Materials and Procedures

Figure 1 shows the detecting module that will be used in the suggested FSO link.

It's a revised form of VIGO System S.A.'s VPAC line of modules..

Figure 1: VPAC series broadband detecting module with biassed photodiode [23].

The standard case of such a module has an infrared photons detector, a four-stage TEC with a temperature sensor, a wideband preamplifier, EMIs, and a little fan dispersing the heat emitted by the cooler. This package also includes a TEC controller and a DC power supply. Figure 2 depicts a schematic diagram of this module.

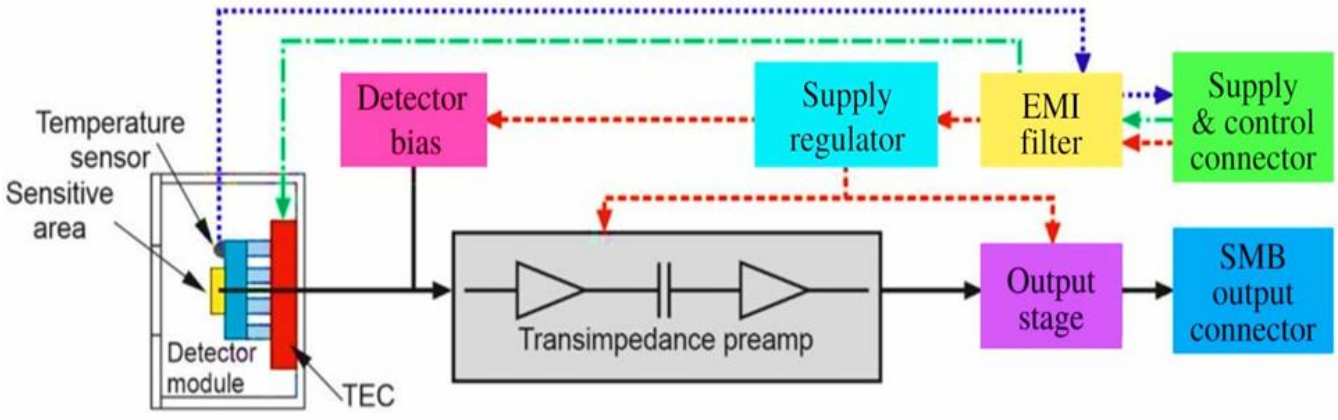

Figure 2: The detection module's block diagram.

TEC stands for thermoelectric cooler; EMI stands for electromagnetic noise filter; and SubMiniature version B connector stands for SubMiniature version B connector (SMB).

Journal of Chemical Health Risks
www.jchr.org
JCHR (2024) 14(4), 2187-2195 | ISSN:2251-6727

The current signal from the HgCdTe photodiode is read by a wideband (about 1 GHz) trans-impedance amplifier. This amplifier also provides a continuous reverse power supply to the detector with a voltage of 200 mV. This prepares the ground for achieving the highest feasible signal-to-noise ratio throughout a wide frequency range. Table 1 lists the most important features of this module, which is built for a wavelength of 10 m. More detailed explanations and experimental studies on the detecting modules represented in Figure 2 can be found in the references [23,24].

Table1.The detection module's basic characteristics were designed for a wavelength range of 10 m [9].

Parameter	**Transimpedance @RLOAD = 50 Ω**	**Output resistance**	**Gain bandwidth**	**Noise voltage**	**Voltage sensitivity**	**Detectivity**
Unit	V/A	Ω	MHz	nV/Hz1/2	V/W	cmHz1/2/W
Value	14.5 × 103	60	0.001÷770	80	2.4 × 105	4 × 1010

The laser was controlled by the LDD 400 module. It features an output that allows you to keep track of how much current is passing through the laser structure. A low-impedance tape was used to link the LLH laser head to the LDD 400 system. The LDD needed to be controlled by an external generator.

The operating temperature of the QC laser was controlled by a TCU 200 controller. A PT100 temperature sensor incorporated into the head was used to measure the temperature. The temperature control range is 40 to +80 degrees Celsius.

Figure 3 depicts the FSO system transmitter module. This module included an optical system, a laser head with a cascade laser, a laser power source, a beam collimating lens, and a water-cooling system.

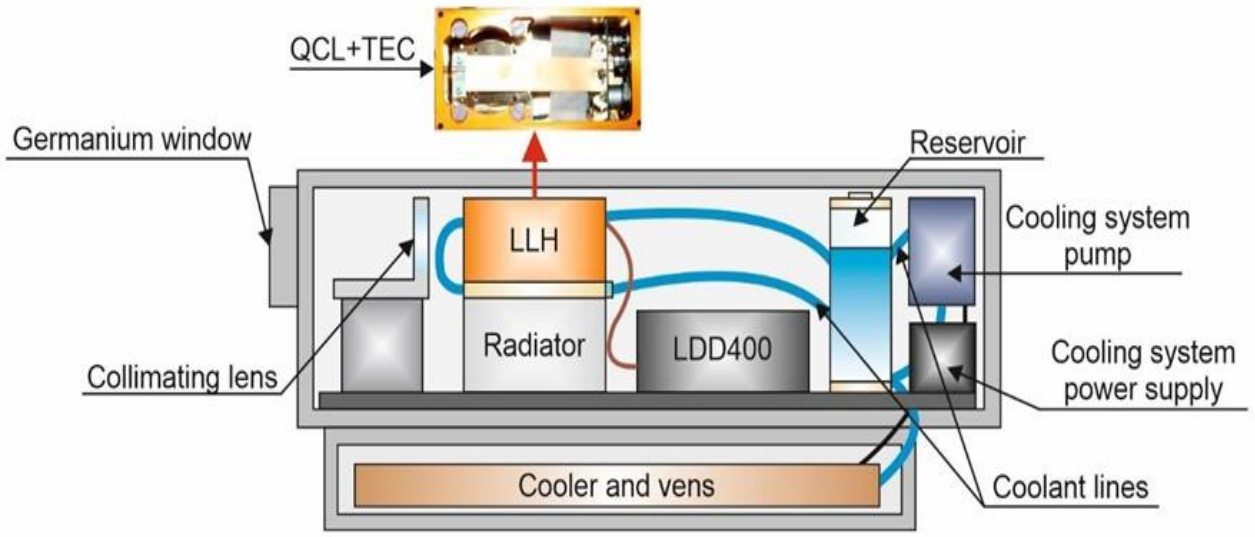

Figure3. FSOmodule.

1. Results

The constructed transmission and reception modules then were employed in the research facility setup shown in Figure 4 as the following stage. They have been on the contrary direction of the lab, close to each other and confronting the mirror. The optical route was approximately 70 metres long. Figure 5 depicts the layout of the lab test stand.

Journal of Chemical Health Risks
www.jchr.org
JCHR (2024) 14(4), 2187-2195 | ISSN:2251-6727

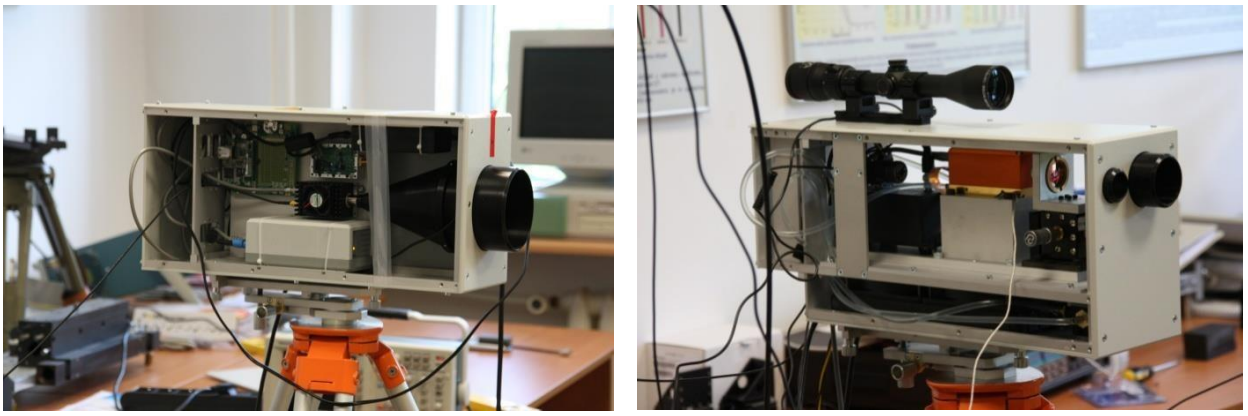

(a) (b)

Figure4.Photo of the FSO link's receiving (a) and transmitting (b) modules

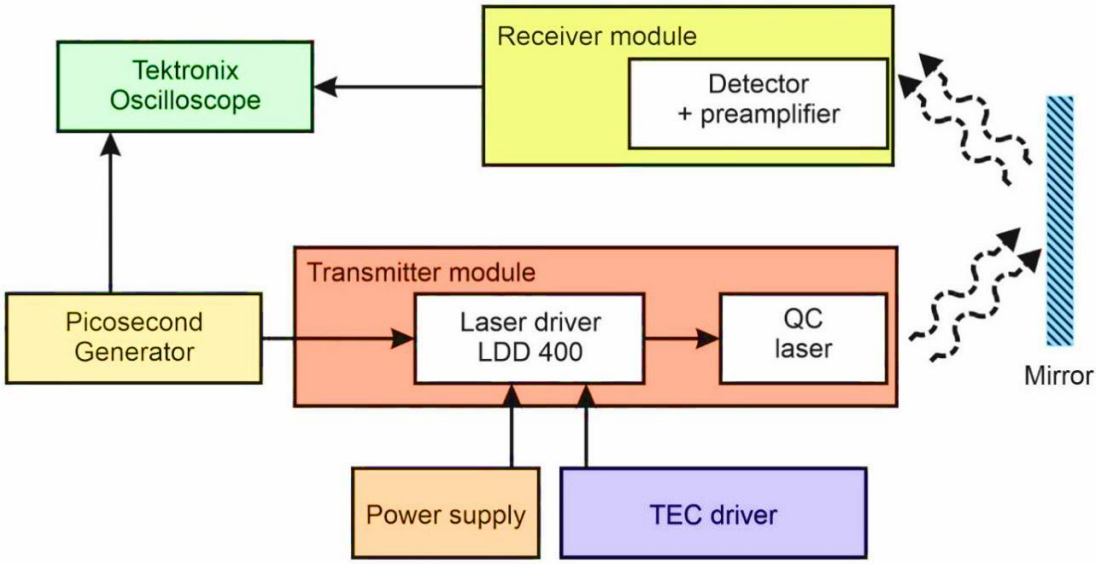

Figure5.The research stance for evaluating the FSO connection under laboratory circumstances is depicted in this diagram. QC stands for quantum cascade and LDD stands for laser diode driver.

The Picosecond 12000 generator was used to create a set of 15000 pseudo-random signals in the RZ code with an intensity of 2.5 V, frequency of 1 MHz, and length of 100 ns to validate the validity of the proposed measuring method. The generator's pulse series was visualised by keeping the captured waveforms in the system storage and scanning the oscilloscope at the same time. The signal average score at logical levels "0" and "1" was then measured, as well as the Q factor, transmission ratio, and RMS noise level at logical levels "0" and "1". The observations were made by limiting the measurement region and using cursors to determine the pulse width.An instance of the oscillogram acquired during the measurements is shown in Figure 6. The approach for determining individual signal characteristics was also checked.

The coefficients of the Q and S/N indices were obtained from the oscillogram. They are, correspondingly, 4.918 and 91.05. The data analysis revealed that when the gating was turned on, the value of the Q factor was compatible with the value calculated using the formula [37]:

Journal of Chemical Health Risks
www.jchr.org
JCHR (2024) 14(4), 2187-2195 | ISSN:2251-6727

Figure6.Bit error rate (BER) measurements resulted in this sample oscillogram.

The influence of the light beam repetition rate, the pulse cycle frequency, and the laser working temp on the BER value was tested using a Picosecond 12,000 generator. Table 2 shows the characteristics of the produced pulses. The study generator allowed for the creation of a pseudo-random series of bits in the device's system storage. As per the previously made pseudo-random series, pulse waveform with a specific frequency, length, and intensity were produced at the induction generator.

Table2.The BER experiments were conducted on the parameters of the pulses generated by the Picosecond 12,000 generator.

Parameter	**Type of work**	**The length of the generated code**	**Character length**	**Code type**	**Pulse frequency**	**Pulse duty cycle**	**Operating temperature of the laser**	**Low-level voltage**	**High-level voltage**
Value	Pseudo-random sequence	14,000 bits	15	RZ (return to zero)	from 450 kHz to 8.0 MHz	from 0.6% to 50%	from −15 ◦C to 25 ◦C	5.5 V	0 V

The computed BER relationships for various pulse power levels, bandwidth values, and laser working temperatures are shown in Figures 7–9.

Journal of Chemical Health Risks
www.jchr.org
JCHR (2024) 14(6), 1840-1843 | ISSN:2251-6727

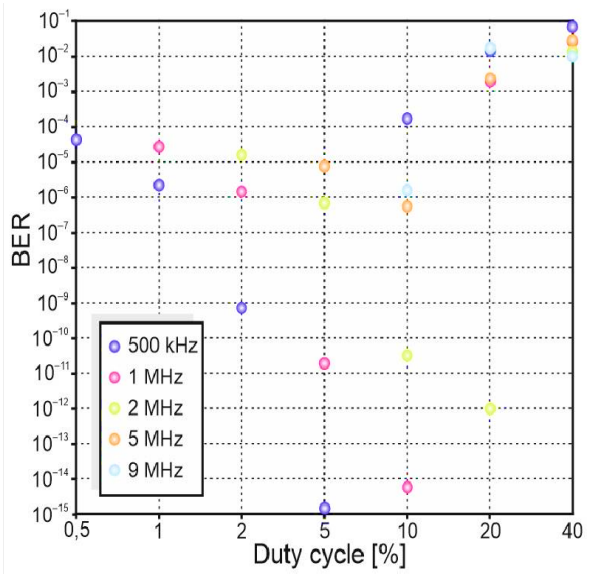

Figure7.At a laser working temperature of 10°C, BER values for various pulse duty factors and frequency were calculated.

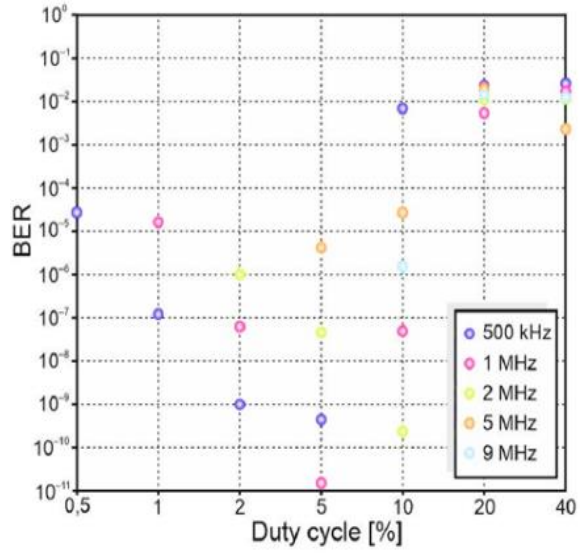

Figure8.BER values for various pulse duty factors and frequency were calculated at a laser operating temperature of 0°

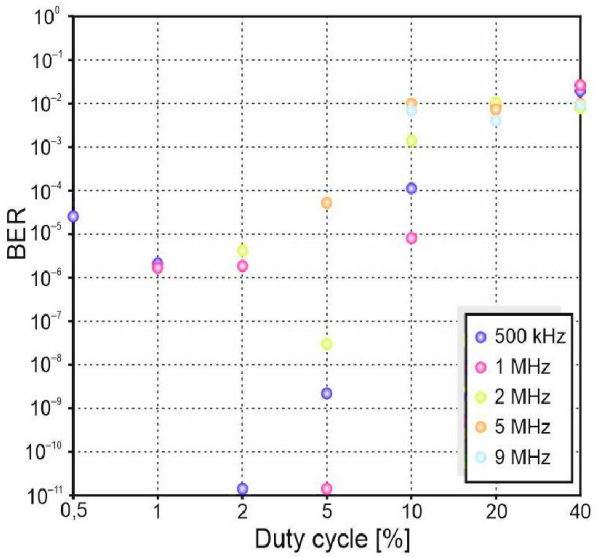

Figure9.BER values for various pulse duty factors and frequency were calculated at a laser working temperature of 20°C.

The minimal BER value was attained with shorter pulse lengths as the laser working temperature rises. The influence behavioral and noise rise at the logical "1" level are caused by the warming of the laser component during long-duration production.

An increase in the variation of the frequency of the pulses was seen as the working heat of the laser increased. It's owing to the QC structural heating during flow of current, and also the shift in operational conditions caused by the cooling system's low effectiveness. Raising the laser working temperature causes a further fall in loudness and a rise in the distortion value, in addition to increasing the pulse width. The link working point is determined by a trade-off between the needed amplitude, frequency, and noise level.

Two observation tracks are used in the experimental testing of the suggested FSO system in real-world situations. The first with the planned link, and the second with a laser that generates 1.5 m wavelength light. The third path, which used a laser to generate 550 nm wavelength photons, has been used to determine accessibility. A digital thermometer was used to determine the temp, and a hygrometer was used to determine the relative moisture. Figure 10 shows a diagram of the study stand used to investigate the impact of meteorological pressure on link operation.

Journal of Chemical Health Risks
www.jchr.org
JCHR (2024) 14(6), 1840-1843 | ISSN:2251-6727

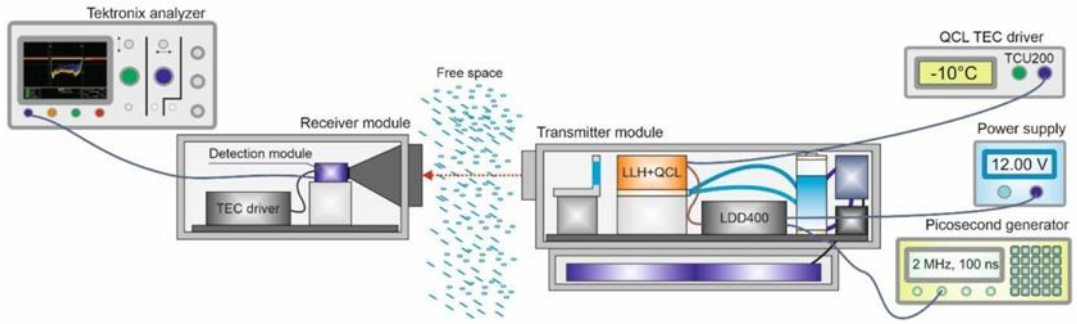

Figure10.The measurement scheme for the FSO link in real-world situations.

Figure 11 depicts the circumstances under which the test was conducted. The link was roughly 80 metres long and ran from side to side across the Military University of Technology. Figure 12 depicts the results of experiments conducted in light hazy conditions: the air temperature was 10 degrees Celsius, and the humidity levels was 100 percent.

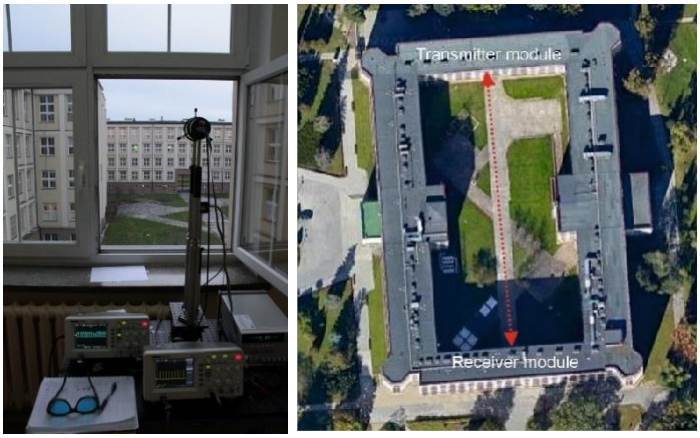

Figure 11.Outside the Military University of Technology building, the laboratory is used to test the FSO link.

Every 20 minutes, the intensity of the signals at the photoreceivers' source was measured. The obtained results were matched to the analytical calculations performed in the earlier article [38] using the MathCAD software. The formula incorporating the transmission factor, propagation duration, and extinction coefficient [39] as well as the relation between humidity and liquid sedimentation signal [40] are used in these computations. The calculations revealed that the present FSO systems, which employ lasers to generate radiation at wavelengths of 800–900 nm and 1.5 m, were sensitive to inclement weather, notably fog. The connection operating with a frequency of 10 m was characterised by a range of 1 km, which equates to light fog.As a result, in the case of limited sight, light with a frequency of 10 m has higher transmission qualities than near-infrared wavelengths. The observed attenuation, considering the diffraction pattern, is similar for the three examined wavelengths for visibility under 600 m . This means that in bad weather, with drastically reduced vision, all systems will have trouble maintaining adequate communication reliability, and there may well be issues establishing a connection. In addition, compared to the short light, radioactivity with a frequency of 10 m is less susceptible to disturbance in the atmosphere.

Journal of Chemical Health Risks

www.jchr.org

JCHR (2024) 14(6), 1840-1843 | ISSN:2251-6727

The absorption of both wavelengths rose as visibility decreased. The absorption of light in the far-infrared band was roughly 10 dB/km for a visibility of 800 m with a small haze, while in the near-infrared region was around 15 dB/km. As shown in Figure 12, the acquired analysis results were equivalent to the experimental results.

Discussion

An FSO system operating in the third-atmosphere propagation window (8–12 m) was presented in this research. According to our research, in the event of severe weather, the proposed link can successfully maintain the connection's continuity. The impact on signal transmission and the location of the disturbance source within the cylinder was discussed in Reference [41]. The FSO analysis in tropical climate was explored in Reference [42], while the experiment in the Mediterranean weather area around the city was seen in Reference [43]. The efficiency of FSOs in the marine sector was examined in Reference [44]. It was proposed to use a computational formula of signal strength that took into consideration a single-point measurement technique for atmospheric characteristics.

Reference [45], on either hand, looked examined the impact of air turbulence's temporal and spatial features. Temporal traits were found to be slightly greater than spatial ones. It is vital to provide a large bandwidth to ensure optimal signal quality as spatial features increase.

The findings of this study show that the suggested FSO link performs as expected both in the lab and in real-world situations. The experimental data were contrasted to the theoretical predictions, which took into consideration the weather systems. Individual wavelengths had identical attenuation levels, which was surprising.

Conclusion:

Turbulence issues could be decreased by improving the links. There are numerous research projects focusing on beam management and tracking strategies for reducing the negative impacts of angle-of-arrival fluctuation and aiming error on the efficiency of free-space optical communications. Automatic resuming of packet trans-mission, adaptable types, multi-beam systems, or adaptive optics structures are also employed to boost system reliability in settings where birefringence or roughness of the atmosphere might cause signal fading.

To summarise, the findings revealed that optical radiation with a wavelength of around 10 m had higher transmission qualities in the presence of limited visibility than near-infrared waves.

Reference:

1. Hamza, Abdelbaset S., Jitender S. Deogun, and Dennis R. Alexander. "Classification framework for free space optical communication links and systems." *IEEE Communications Surveys & Tutorials* 21.2 (2018): 1346-1382.

2. Huang, Qingchao, et al. "Secure free-space optical communication system based on data fragmentation multipath transmission technology." *Optics express* 26.10 (2018): 13536-13542.

3. Huang, Xu-Hong, et al. "WDM free-space optical communication system of high-speed hybrid signals." *IEEE Photonics Journal* 10.6 (2018): 1-7.

4. Wang, Wei-Chun, Huai-Yung Wang, and Gong-Ru Lin. "Ultrahigh-speed violet laser diode based free-space optical communication beyond 25 Gbit/s." *Scientific reports* 8.1 (2018): 1-7.

5. Yin, Xiaoli, et al. "Adaptive turbulence compensation with a hybrid input–output algorithm in orbital angular momentum-based free-space optical communication." *Applied optics* 57.26 (2018): 7644-7650.

6. Shao, Wei, et al. "Free-space optical communication with perfect optical vortex beams multiplexing." *Optics Communications* 427 (2018): 545-550.

7. Cox, Mitchell A., et al. "Modal diversity for robust free-space optical communications." *Physical Review Applied* 10.2 (2018): 024020.

8. Sakthivel R., Sundareswari K., Mathiyalagan K., Arunkumar A., Anthoni S.M.” Robust reliable H∞ control for discrete-time systems with

Journal of Chemical Health Risks

www.jchr.org

JCHR (2024) 14(6), 1840-1843 | ISSN:2251-6727

actuator delays" *Asian Journal of Control* (2015).

9. Mai, Vuong V., and Hoon Kim. "Adaptive beam control techniques for airborne free-space optical communication systems." *Applied Optics* 57.26 (2018): 7462-7471.
10. Mathew O.C., Rahman A.M.J.Z." A novel energy optimization mechanism for medical data transmission using honeycomb routing" *Journal of Medical Imaging and Health Informatics* (2016).
11. Tan, Jun, et al. "12.5 Gb/s multi-channel broadcasting transmission for free-space optical communication based on the optical frequency comb module." *Optics express* 26.2 (2018): 2099-2106.
12. Arikawa, Manabu, and Toshiharu Ito. "Performance of mode diversity reception of a polarization-division-multiplexed signal for free-space optical communication under atmospheric turbulence." *Optics express* 26.22 (2018): 28263-28276.
13. Jaiswal, Anshul, and Manav R. Bhatnagar. "Free-space optical communication: A diversity-multiplexing tradeoff perspective." *IEEE Transactions on Information Theory* 65.2 (2018): 1113-1125.
14. Yeh, Chien-Hung, et al. "Hybrid free space optical communication system and passive optical network with high splitting ratio for broadcasting data traffic." *Journal of Optics* 20.12 (2018): 125702.
15. Khader, Isaac, et al. "Time synchronization over a free-space optical communication channel." *Optica* 5.12 (2018): 1542-1548.
16. Dabiri, Mohammad Taghi, Seyed Mohammad Sajad Sadough, and Mohammad Ali Khalighi. "Channel modeling and parameter optimization for hovering UAV-based free-space optical links." *IEEE Journal on Selected Areas in Communications* 36.9 (2018): 2104-2113.
17. Huang, Guan, et al. "Adaptive SMF coupling based on precise-delayed SPGD algorithm and its application in free space optical communication." *IEEE Photonics Journal* 10.3 (2018): 1-12.